HHS Public Access

Author manuscript

*Hypertension*. Author manuscript; available in PMC 2021 December 01.

Published in final edited form as:

*Hypertension*. 2020 December ; 76(6): 1847–1855. doi:10.1161/HYPERTENSIONAHA.120.15939.

# Microbiota introduced to germ-free rats restores vascular contractility and blood pressure

**Bina Joe**, **Cameron G. McCarthy**, **Jonnelle M. Edwards**, **Xi Cheng**, **Saroj Chakraborty**, **Tao Yang**, **Rachel M. Golonka**, **Blair Mell**, **Ji-Youn Yeo**, **Nicole Bearss**, **Janara Furtado**, **Piu Saha**, **Beng San Yeoh**, **Matam Vijay-Kumar**, **Camilla F. Wenceslau**

UT Microbiome Consortium, Center for Hypertension and Precision Medicine, Department of Physiology and Pharmacology, University of Toledo College of Medicine & Life Sciences, Toledo OH, USA.

## Abstract

Commensal gut microbiota are strongly correlated with host hemodynamic homeostasis, but only broadly associated with cardiovascular health. This includes a general correspondence of quantitative and qualitative shifts in intestinal microbial communities found in hypertensive rat models and human patients. However, the mechanisms by which gut microbes contribute to the function of organs important for blood pressure control remain unanswered. To examine the direct effects of microbiota on blood pressure, we conventionalized germ-free (GF) rats with specific pathogen free rats for a short-term period of 10 days, which served as a model system to observe the dynamic responses when reconstituting the holobiome. The absence of microbiota in GF rats resulted with relative hypotension compared to their conventionalized counterparts, suggesting an obligatory role of microbiota in blood pressure homeostasis. Hypotension observed in GF rats was accompanied by a marked reduction in vascular contractility. Both blood pressure and vascular contractility were restored by the introduction of microbiota to GF rats, indicating that microbiota could be impacting blood pressure through a vascular-dependent mechanism. This is further supported by the decrease in actin polymerization in arteries from GF rats. Improved vascular contractility in conventionalized GF rats, as indicated through stabilized actin filaments, was associated with an increase in cofilin phosphorylation. These data indicate that the vascular system senses the presence (or lack of) microbiota to maintain vascular tone via actin polymerization. Taken together, these results constitute a fundamental discovery of the essential nature of microbiota in blood pressure regulation.

## Graphical Abstract

**Corresponding authors:** Camilla Ferreira Wenceslau, Ph.D., Camilla.Wenceslau@utoledo.edu, Bina Joe, Ph.D., Bina.Joe@utoledo.edu, Department of Physiology and Pharmacology, University of Toledo College of Medicine & Life Sciences, 3000 Transverse Drive, Toledo, Ohio 43614-2598, Phone#: 419.383.5307.

Disclosure

None.

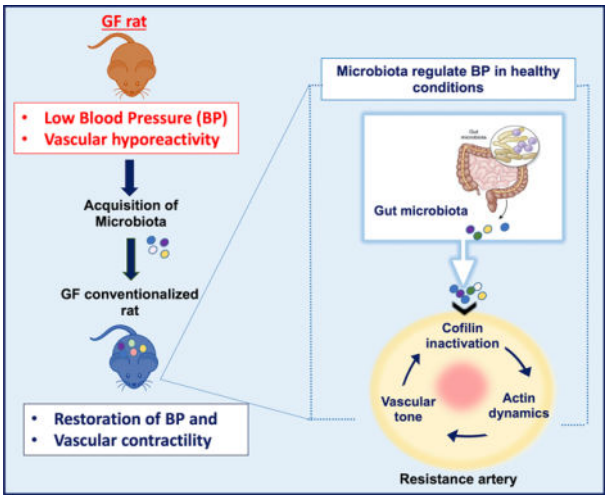


**Keywords**

Microbiota; blood pressure; actin polymerization; vascular contraction

## Introduction

Despite the increasing awareness and treatment options for elevated blood pressure (BP), hypertension is still escalating at an unprecedented rate, and is sure to surpass the projections of estimated incidences expected for 2025[1]. In the United States, hypertension prevalence is near 50% of the adult population[2] and the incidence rate in children is climbing correspondingly[3]. Considerable genetic research has highlighted the importance of polymorphic variants in the etiology of hypertension, many of which have been modeled in animals[4–8]. In genetically predisposed individuals, early exposure to various environmental factors can trigger later onset hypertension development[9]. A non-genetic, yet heritable, contributor to BP regulation may be the microbiota. Microbiota are mainly harbored in our distal gastrointestinal tract, but also in other anatomical regions such as on the skin and in our mouth. We and others have shown that reconfiguration of the microbiota (i.e. high sodium diet, antibiotics) can alter metabolic and immunological functions, which can subsequently induce changes to host homeostasis and/or causes alterations that become inherited by its offspring[10,11]. In addition, transplantation of microbiota from hypertensive rodents or humans to animal models with normal BP can recapitulate hypertension[12,13].

Microbiota composition in human hypertensive patients are different from normotensive individuals[12], and gut microbiota dysbiosis contributes to the development of hypertension[13,14]. Thus, there is considerable focus on understanding how a reshaped gut microbiota contributes to the adverse transition from normal BP to a hypertensive state[10,14]. However, these studies do not address the fundamental question of whether microbiota are an essential component of host BP regulation. This premise arises from our understanding that humans have co-evolved with microbiota as ‘holobionts’, whereby we are dependent on the microbiota for many imperative functions. Since BP is one such vital physiological index of host health, it is important to understand if we need microbiota for maintaining

hemodynamic health. Herein, we sought to define the contributions of the microbiota on host BP regulation by utilizing incomplete holobionts, as represented by germ-free (GF) rats, and conventionalized GF rats (GFC) that characterize the reconstituted, complete holobiont. We found that co-housing GF rats with conventional (germ-full) rats for 10 days was sufficient to rescue and regain BP homeostasis in hypotensive GF rats. Vascular contractility and actin polymerization, which were decreased in the GF rats suggesting a plausible mechanism for the hypotension in GF rats. We propose that the microbiota are an essential factor required to maintain BP homeostasis via the stabilization of vascular contractility.

## Methods

The data that support the findings of this study are available from the corresponding author upon reasonable request.

### Animals

Male, 7-week-old Sprague Dawley (SD) rats (inbred) that were either germ-free (GF) or germ-free conventionalized (GFC, *alias* 'germ full') (n=6/group) from Taconic Biosciences (Rensselaer, NY) were used for this study. Conventionalization of GF rats was performed by co-housing GF rats with conventionally raised rats (outbred) for 10 days (1:1 ratio). This allowed GF rats to receive a natural, continuous infusion of microbiota via coprophagy. Upon arrival at the University of Toledo, the animals were immediately used for experiments. All procedures were performed in accordance with the Guide for the Care and Use of Laboratory Animals[15] and were reviewed and approved by the Institutional Animal Care and Use Committee of the University of Toledo College of Medicine and Life Sciences, Toledo, OH.

### Blood Pressure (BP) measurements

Although we acknowledge that radiotelemetry is the preferred method to monitor rodent BP, this method was not feasible for our studies because it would jeopardize the 'incomplete holobiont' status of the GF rats. Therefore, *in lieu* of telemetry, systolic and diastolic BP were measured by the tail-cuff method (CODA™ High Throughput System, Kent Scientific Corporation, USA), aseptically in a biosafety hood immediately prior to euthanasia. Data were obtained as the average of the 8–10 successive measurements.

### Morphological parameters of cardiac and non-cardiac tissues

The animals were killed by quick excision of the heart under continued deep anesthesia (5% isoflurane). Rapid excision and careful removal of cardiac and non-cardiac tissue was performed. The total heart, left (LV) and right (RV) ventricles weights were measured and normalized, as previously described[16]. Briefly, it has been shown that body weight correlated linearly (cubically) with tibia length ($TL^3$)[16]. The linear equation of heart weight crossed the x-axis at $TL^3 = -27.7^3$ (95% CI $-30.6^3$; $-24.8^3$), LV weight crossed the x-axis at $TL^3 = -26.7^3$ (95% CI $-29.8^3$; $-23.4^3$), and RV weight at $TL^3 = -26.5^3$ (95% CI $-29.0^3$; $-22.2^3$)[16]. For optimal indexing by TL, the heart weight, LV weight, and RV weight were indexed by dividing the weights by $27.7^3 + TL^3$, $26.7^3 + TL^3$, and $26.5^3 + TL^3$, respectively.

Kidneys, spleen, and cecum weights were also normalized by TL. It is well established that GF animals have ceca which, with their contents, weigh about six times than that of conventional animals[17]. Alongside, total white adipose tissue (WAT) was excised and weighed and mesenteric vascular bed was removed to investigate isolated resistance artery function.

### 16S ribosomal RNA (rRNA) gene sequencing and analysis of microbiota composition

As previously described[11], fecal DNA was extracted from one fecal pellet (~0.2 g). For PCR library preparation, 16S rRNA gene sequencing and analysis, the V3 to V4 regions of the 16S rRNA gene were amplified following the Illumina User Guide: 16S rRNA gene Metagenomic Sequencing Library Preparation - Preparing 16S Ribosomal RNA Gene Amplicons for the Illumina MiSeq System (Illumina, Part # 15044223 Rev. B; Illumina, San Diego, CA)[11]. The 10 pmol/L denatured and diluted library with 15% PhiX was loaded on an Illumina MiSeq V3 flow cell kit with 2×300 cycles. Raw paired-end reads of the 16S sequencing data were merged to create consensus sequences and then quality filtered using USEARCH[18](version 9). Chimeric sequences were identified and filtered using the QIIME software package (version 1.9.1)[19] combined with the USEARCH (version 9) algorithm. Operational taxonomic units (OTUs) were subsequently picked using QIIME combined with the USEARCH (version 9) algorithm, and taxonomy assignment was performed using Greengenes[20] as the reference database.

### 16S rRNA Gene Copy Number Quantification

Internal standard (IS) was designed from E. coli 16S ribosomal RNA gene sequence (GenBank: J01859.1) deleting 10–15% sequences of target regions. The IS was cloned in a vector (Thermo Fisher Scientific, Inc. Waltham, MA), purified after running on agarose gel for a right size of band, purified with QIAquick Gel Extraction Kit (Qiagen), quantified the copy number of IS based on molarity by Bioanalyzer 2100 (Agilent), and serially diluted with low TE buffer (0.1mM EDTA, Tris-HCl, pH 8.0 containing 0.1μg/μl salmon sperm carrier DNA) from 10–11M (6,000,000 copies) to 10–16M (60 copies). To determine the true concentration of IS, limiting dilution PCR and Poisson analysis were used as previously described[21].

To quantify bacterial copy number of 16S rRNA gene native template (NT), a competitive PCR with IS was performed in a 25 μl volume including 2.5 μl DNA, 1 μl IS, 1μl of 5 μM primers mix (same sequences above), and 12.5 μl AccuStart II PCR ToughMix® (Quantabio, Beverly, MA) with 8 μl water. Cycle parameters were 95°C for 3 min, then 35 cycles at 95°C for 30s, 55°C for 30 s, and 72°C for 30 sec, and holding at 72°C for 5 min. An amplified product was run on Bioanalyzer to compare two peaks of IS and NT area under the curve (AUC). For calculation of target copy number, NT AUC was corrected by multiplying the ratio of expected size (i.e., IS/target: 467bp/525bp), and then compared by known number of input IS by following formula:

$$(\text{known copy of input IS}):(\text{unknown NT}) = (\text{IS AUC}):(\text{corrected NT AUC}).$$

### Vascular function

After careful removal of the mesenteric arterial arcade, third-order branches from mesenteric arteries were removed and cleaned of surrounding perivascular adipose tissue in cold Krebs-Henseleit solution (KHS, in mmol/L: NaCl, 130; KCl, 4.7; $NaHCO_3$, 14.9; $CaCl_2.2H_2O$, 1.6; $KH_2PO_4$, 1.2; $MgSO_4.7H_2O$, 1.2; EDTA, 0.03; glucose, 5.6; pH 7.4). Segments of 2 mm in length were mounted in wire myograph chambers (Danish Myo Tech, model 610M; JP-Trading I/S) for isometric tension recordings, as described previously[22,23]. Briefly, two tungsten wires (40 μm diameter) were introduced to resistance arteries through the lumen of the segments and mounted according to the method described by Mulvany and Halpern[24]. After a 15-min equilibration period in oxygenated KHS at 37°C, segments were stretched to their optimal lumen diameter for active tension development. This was determined based on the internal circumference/wall tension ratio of the segments by setting the internal circumference, $L_0$, to 90% of what the vessels would have been if they were exposed to a tension equivalent to that produced by a transmural pressure of 100 mmHg (L100)[22,23]. The diameter (I1) was determined according to the equation $I1 = L1/\pi$ using specific software for normalization of resistance arteries (DMT Normalization Module; ADInstruments). Segments were washed with KHS and left to equilibrate for another 20 min. Vessel contractility and endothelium viability were then tested by an initial exposure to a high potassium chloride solution (KCl,120 mmol/L), followed by acetylcholine (3 μmol/L) in arteries that were contracted previously with phenylephrine (10 μmol/L), respectively. Arteries rested for 30 min after which they were subjected to each of the following three protocols: 1) concentration-response curves to phenylephrine (1 nmol/L to 100 μmol/L); 2) concentration-response curves to acetylcholine (1 nmol/L to 10 μmol/L); and 3) concentration-response curves to sodium nitroprusside (1 nmol/L to 10 μmol/L).

### Enzyme Immunoassay for the quantitative determination of adrenaline (epinephrine) and noradrenaline (norepinephrine).

Arterial blood was collected from the abdominal aorta in tubes containing heparin. Blood was immediately centrifuged at 1500 g for 15 min at 4°C. Plasma was then stored in multiple aliquots at −80 °C until analysis. Enzyme immunoassay [2-CAT (A-N) Research ELISA, Labor Diagnostika NORD GmbH & Co. in Nordhorn, Germany, purchased through Rocky Mountain Diagnostics, Inc in Colorado Springs, CO. Product # BA E-5400] was used to measure epinephrine and norepinephrine. For this, 8 μl of sample (in duplicate) was pipetted into microtiter strips and the antigen was bound to the solid phase of the plate. The antibody bound to the solid phase is detected by an anti-rabbit IgG-peroxidase conjugate using TMB (3,3', 5,5"-tetramethylbenzidine) as a substrate. The reaction is monitored at 450 nm. Nonlinear regression analysis was done using elisaanalysis.com.

### Cell culture, migration and proliferation assays using live-cell analysis systems

Thoracic aortae and primary vascular smooth muscle cells (VSMCs) were isolated and cultured using an enzymatic digestion method, as previously described[23]. VSMCs were then grown in a humidified chamber at 37°C, with 5% $CO_2$, and low glucose Dulbecco's Modified Eagle's Medium (GE Healthcare, Logan, UT, USA) containing 10% fetal bovine serum and 1% penicillin/streptomycin solution (Corning, Manassas, VA, USA). Cell

migration was evaluated via scratch wound and ClearView Chemotaxis assays to allow continuous invasion, monitoring, and analyzing of cell migration without a chemotactic gradient. Cell proliferation was measured via IncuCyte by analyzing the occupied area (% label-free confluence) of cell images over time. For scientific rigor, the cells were used at passage 2–3. Also, the day prior to cell proliferation analysis, VSMCs were plated at a density of 8000 cells per well. As positive control and comparative purpose, we used aortic VSMCs from male, 7-week old Sprague Dawley (SD) conventional rats.

### Filamentous and globular actin quantification

The most accurate method of determining the amount of filamentous actin (F-actin) content versus free globular actin (G-actin) content in a cell population is to quantify F-actin and G-actin cellular fractions[23]. VSMCs were processed according to a G actin: F actin *in vitro* assay (Cytoskeleton, USA). Briefly, VSMCs were lysed in a detergent-based buffer that stabilizes the G and F forms of actin. Ultracentrifugation was then used to separate the G actin into the supernatant while pelleting the F actin. After collecting the G actin, the F actin was depolymerized. Finally, the F and G actin samples were loaded into polyacrylamide gels (10%), separated by sodium dodecyl sulfate polyacrylamide gel electrophoresis (SDS-PAGE), and transferred to nitrocellulose membranes, as described below for immunoblotting (Cytoskeleton, USA). Densitometric analysis was performed by ImageJ.

### Immunoblotting

In another set of experiments, we used aortic VSMCs from male GF, GFC and SD rats (positive control) to understand actin dynamics. Cells were washed with an ice-cold phosphate-buffered saline (PBS) solution. Complete Lysis-M, including phosphatase inhibitor cocktail (PhosSTOP) (both Roche, Indianapolis, IN, USA), was then applied to each plate and allowed to remain on ice for 30 min. Cells were then harvested. Protein concentration was first determined and then equal quantities of protein (25 or 50 μg) were loaded into polyacrylamide gels (8–12%), separated by SDS-PAGE, and then transferred to nitrocellulose membranes. The membranes were blocked with 5% nonfat dry milk and incubated overnight at 4°C with primary antibodies raised against anti-phospho-cofilin ($pSer^{3}$) (1:1000), anti-cofilin (1:1000) anti-phospho-vasodilator-stimulated phosphoprotein (VASP, $pSer^{239}$) (1:000), anti-VASP (1:000), anti-alpha-1a adrenergic receptor (ADRA1A; 1:500), anti-phospho myosin phosphatase target subunit 1 Threonine 696 (MYPT1; 1:1000), anti-MYPT1 (1:1000); anti-phospho-p44/42 MAPK (Erk1/2) (Thr202/Tyr204), anti-ERK 1/2 (1:1000) and β-actin (1:40,000). Densitometric analysis was performed by ImageJ. Antibodies: phospho- and total-cofilin, VASP, MYPT-1 and ERK were purchased from Cell signaling. β-actin was purchased from Sigma. ADRA1A was purchased from Invitrogen-ThermoFisher Scientific.

### Bioenergetic Assays

We used the Agilent Seahorse XF Cell Mito Stress Test to measure key mitochondrial function parameters by direct measurement of the oxygen consumption rate (OCR) and extracellular acidification rate (ECAR) of VSMCs on the Seahorse XF96 Analyzer. The day prior to the assay, VSMCs (passage 2) were plated at a density of 8000 cells/80 μL into a 96 well Seahorse XF Cell Culture Microplate. The XF96 sensor cartridge was hydrated in

Seahorse XF Calibrant at 37°C in a non-$CO_2$ incubator overnight. The plate was mapped for the VSMCs of each individual animal in triplicates. On the day of the assay, Seahorse XF DMEM was supplemented with 1 mM pyruvate, 2 mM glutamine, and 10 mM glucose. The drugs oligomycin (an ATP synthase inhibitor, 1.5 μmol/L), carbonyl cyanide-4 (trifluoromethoxy) phenylhydrazone FCCP (an ionophore, which shuttles hydrogen ions, 1 μmol/L) and Rotenone/Antimycin A (an electron transport chain complex I and III inhibitors, respectively, 0.5 μmol/L) were added sequentially by the Seahorse XF96 analyzer to assess mitochondrial respiration. Hoechst 33342 nuclear staining dye (20 μM) was mixed with the Rotenone/Antimycin A mixture to allow for post-assay fluorescent image captures with the BioTek Cytation 5 (BioTek Instruments, Winooski, USA). Subsequent cell counting for data normalization was performed by using Fiji, an image processing focused distribution of ImageJ.

### Pharmacological agents

Stock solutions of phenylephrine, acetylcholine and sodium nitroprusside were prepared freshly in sterile and distilled water. All chemicals were purchased from Millipore-Sigma (Saint Louis, USA).

### Statistical analyses

The statistical procedures used included Student's unpaired t-tests, one and two-way analysis of variance (ANOVA). Wilcoxon rank sum test was used to compare bacterial 16S gene copy number between GF and GFC rats. For concentration-response curves, maximum response (efficacy or E*max*) was calculated to show the highest point on the curve. Half maximal effective concentration ($EC_{50}$) was calculate to evaluate potency of the drug in case no differences were observed in Emax between curves. All analyses were performed using data analysis software GraphPad Prism 8.0. Number (n) of the animals used is indicated in the graphs. Statistical significance was set at $p<0.05$. The data are presented as mean ± SEM.

## Results

### Germ-free rats exhibit lower blood pressure compared to conventionalized rats

High amount of microbiota was detected in the fecal samples of GFC rats compared to GF rats that was similar amount of no template control samples on library preparation of 16S rRNA gene sequencing (Figure 1A). To our knowledge, germ-free animals are free of any 'viable' bacteria, but are still susceptible to receive bacterial DNA (dead ones) through the autoclaved diet[25,26]. As previously described, small amount of 16S in the fecal samples from GF is from the diet, which despite autoclaved, still have trace amounts of bacterial DNA[25,26]. However, this is usually negligible or only detected in very small trace amount as observed in Figure 1A. Another common source of 'contamination' (dead bacteria) may be from the sterilized equipment, and steps in sample processing, where tubes and reagents can also introduce some small number of 16S in the fecal samples.

16S rRNA sequencing analysis also confirmed successful colonization of 9 bacterial phyla (43% Bacteroidetes; 38% Firmicutes; 10% Proteobacteria; 7% Verrucomicrobia; 1%

Actinobacteria; 1% Cyanobacteria; <1% Deferribacteres; <1% TM7; <1% Teneticutes) in the GFC rats, as described by Yang et al.[27]. The lack of microbiota in GF rats was associated with an increase in their cecum weight compared to GFC rats (Figure 1B and C). Kidney and spleen weights were unaltered between the groups (Table 1). However, body weight and white adipose tissue (WAT) were lower in GF rats (Table 1). Both systolic and diastolic BP of GF rats were significantly lower than that of GFC rats (Figures 2A, B and C). Further, total heart and left ventricular (LV), weights were all lower in GF rats compared to GFC rats (Figures 2D and E), and this was only a trend in the right ventricular (RV) (Figure 2F).

### Reconstituting the microbiota improved vascular contractility in conventionalized rats

To assess the contribution of the colonized microbiota on vascular function, we measured isometric force in mesenteric resistance arteries (diameter < 300 μm) from GF and GFC rats. The absence of commensal microbiota decreased both KCl and phenylephrine-induced contraction in GF rats (Figures 3 A–C; Table S1). No differences were observed in endothelium-dependent and independent relaxation (Figures 3 D and E, Table S2), nor changes in lumen diameter (Table S1). Given the undisputable role of vascular tone in maintaining and control BP, these data suggest that the hyporesponsive vasculature of GF rats could contribute to the observed lowering of BP compared to the GFC rats.

### Absence of microbiota did not affect plasma levels of adrenaline (epinephrine) and noradrenaline (norepinephrine)

Since plasma epinephrine and norepinephrine concentrations are important to maintain vascular tone and control blood pressure, we questioned if plasma levels of these catecholamines would be decreased in GF rats and reconstitution of microbiota would restore these parameters. No changes were observed in epinephrine and norepinephrine between groups (Figures 4 A and B). It is important to emphasize that these measurements were performed in the basal state, which does not exclude the possibility that the plasma levels of catecholamines would be different between groups in response to stimuli that either increase or decrease sympathetic activity.

To understand if the low contraction to phenylephrine in arteries from GF rats would be due to a reduction in alpha-1a adrenergic receptor (ADRA1A), we measured ADRA1A protein expression in the VSMC from all groups. No changes were observed in ADRA1A protein expression between groups (Figures 4 C and D). Overall, these data suggest that other(s) mechanism (s) different than sympathetic activity, play a role in the hyporesponsive vasculature of GF rats.

### Absence of microbiota reduces vascular actin polymerization

Given that arteries from GF rats presented a reduction in contractility, we hypothesized that cytoskeletal dynamics deficits are a likely cause for the observed reduction in vascular contraction. Therefore, we examined actin dynamics by measuring actin polymerization in VSMCs from GF and GFC rats. Filamentous actin was less pronounced in GF rats compared to positive control (Figure 4 E and F). No differences were observed in F: G actin ratio between GFC and positive control (Figure 4 E and F). These suggest that reconstitution of microbiota in the GFC rats partially increase actin polymerization via a shift in the F: G

equilibrium in favor of F-actin, *albeit* not significantly compared to GF (Figure 4 E and F). Additionally, these data also indicate that the hyporesponsive vascular phenotype of GF rats is, at least in part, due to intrinsic changes in the VSMCs.

Given that actin polymerization requires constant energy consumption, we questioned if low actin polymerization and, subsequently reduced vascular contraction, would be due to mitochondria dysfunction. Further, since actin polymerization is also an anabolic process and the cytoskeleton mechanically regulates glycolysis[28], we measured glycolysis by ECAR and oxidative phosphorylation (through OCR) simultaneously in live VSMCs from GF and GFC rats. A scheme for the overall bioenergetics profile is demonstrated in Figure S1A. We observed that OCR, which represents mitochondria function, is similar between groups (Figure S1B). On the other hand, we found that VSMCs from GF rats presented a reduction in ECAR (a measure for glycolysis) when compared to GFC rats (Figure S1C). Taken together, these data indicate that microbiota are essential for regulating actin polymerization and associated bioenergetic profiles.

## Microbiota promote actin polymerization via inactivation of cofilin

Next, we sought to identify a molecular mechanism contributing to the higher depolymerization of actin in GF rats. We focused on cofilin, a major actin-binding protein that disassembles actin filaments. Specifically, cofilin actively promotes actin depolymerization and phosphorylation inhibits this activity[29]. Phosphorylation of cofilin was significantly lower in the VSMCs of GF rats compared to GFC rats Figures 5 A and B. There were no differences in phosphorylation of another actin polymerization regulator, named VASP (vasodilator-stimulated phosphoprotein), indicating that microbiota specifically induced phosphorylation of cofilin in GFC rats (Figure S2A–C). It has been shown that viral stimulation of phosphor ERK1/2 leads to cofilin phosphorylation and inactivation and, subsequently, F-actin polymerization[30]. Corroborating these data, we observed that absence of microbiota leads to decrease in phospho ERK1/2 (Figure 5 C and D). These data suggest that increased in F-actin depolymerization via activation of cofilin in arteries from GF rats may be due to decreased phospho ERK1/2. Reconstitution of microbiota, similar to the viral stimulation[30], reversed these responses (Figure 5 C and D). In addition to actin polymerization dysregulation, we questioned if a regulatory subunit of myosin light chain phosphatase would regulate vascular tone in arteries from GF rats. No changes were observed in phospho myosin phosphatase target subunit 1 (MYPT1) protein expression between groups (Figures S2 D and E).

Because cell migration and proliferation are driven by continuous reorganization and turnover of the actin cytoskeleton, we measured these parameters in VSMCs from GF and GFC rats. Interestingly, both parameters are reduced in VSMC from GF and GFC when compared to positive control (Figures S3 and S4). These data indicate that the acute exposure of microbiota (10 days) to GF rats increased phosphorylation of cofilin to maintain vascular tone (Figure 5A), but prolonged exposure may be required for the actin polymerization-dependent cellular migration and proliferation (Figures S3 and S4).

## Discussion

Selective pressure during evolution has fostered strategic symbiotic alliances between the host and commensal microbiota. While the host components responsible for mammalian homeostasis have been extensively documented, the dependency of the host on commensal microbes for maintenance of cardiovascular health has been only recently recognized. As relevant to BP homeostasis, it has been shown that gut dysbiosis is associated with hypertension[10,12–14,31]. In line with this, Yang et al.[14] reported microbial dysbiosis in the spontaneously hypertensive rat (SHR), as well as in a small cohort of hypertensive patients, when compared to normotensive rats and humans, respectively[14]. Since then, similar animal studies from other models as well as human studies from diverse cohorts have reported clear differences in microbial compositions between hypertensive and normotensive groups[10,12–14,31]. While these association studies both in animal models and in humans suggest that the microbiome may impact BP, the underlying mechanism(s) showing how a mammalian host requires commensal microbiota to regulate BP is still unclear.

In the current study, we addressed this problem using the experimental design of comparing germ-free (GF) rats to represent the host devoid of the microbial component and conventionalized rats with reconstituted microbiota. We demonstrated that rats lacking microbiota had lower BP and vascular hypocontractility via decreased actin polymerization, which was restored by the acquisition of microbiota. A limitation of our study is that we procured inbred, 7-week-old SD rats that were either GF or re-conventionalized GF (GFC). Re-conventionalization of GFC was performed by co-housing GF rats with outbred conventionally-raised SD rats for 10 days. Although we had SD rats available, as controls, from a genetic point of view, the comparison between physiological parameters, such as vascular function and BP, are not acceptable due to genetic variability between groups which interferes in the interpretation of the data. However, in our previous study, where we used conventional (control) and GF mice[32], we also observed similar phenotype in arteries (hypocontractility) from GF mice. Therefore, this previous study solidified the present null and alternative hypothesis that microbiota restored rat from slight hypotension and lower vascular contractility. Further, in the absence of dysbiosis, microbiota are not pathological in inducing abnormal elevation BP.

As defined by Poiseuille’s law, lumen diameter, vessel length, and viscosity of the blood are the primary determinants of the resistance to blood flow within a vessel. The most significant by far is the lumen diameter, because vessel resistance is inversely proportional to the radius to the fourth power. Therefore, any reduction in vascular tone and contractility would significantly decrease vascular resistance and, subsequently, BP. It is known that prolonged vasoconstriction of resistance and large arteries involves VSMCs actin polymerization[33]. In the present study, one of the mechanisms for the hypocontractile responses in GF rats was traced to defects in the polymerization of actin filaments caused by the activation of cofilin. Interesting, introduction of gut microbiota to GF rats phosphorylated and, consequently, inhibited cofilin. Thus, we suggested that signaling by microbiota are essential for the functional homeostasis of host vasculature. Because vascular function directly controls BP, this newly discovered function of microbiota on VSMC actin polymerization, at least in part, responsible for the underlying mechanism by which

microbiota regulate BP. Although, we did not observe differences in endothelium- dependent and independent relaxation in arteries from GF and GFC rats, it cannot be excluded that a continuous release of an endothelial vasodilator(s) contributes to the difference observed here. Further, two events truly dependent on actin polymerization, migration and proliferation, were decreased in arteries from GF rats, and reconventionalization of the rats did not improve these responses. It is possible that only 10 days of reconventionalization may not be sufficient to recovery these parameters. Also, there is a possibility that other mechanism(s), such as endothelial-derived contractile factors, may play a role in microbiota-induced vascular changes. Finally, although we did not observe differences in circulating catecholamine levels between groups, the effects of sympathetic activity on the vasculature of GF and GFC cannot be completely excluded since our measurements were performed in the basal state. All these inferences will be addressed in future studies.

This is the first report using GF and conventionalized GF rats to study the contributions of microbiota to vascular function and BP regulation. Introducing microbiota for a short duration of 10 days was enough to elicit differential vascular and BP responses, suggesting that microbial factor(s) cause rapid effects on the host cardiovascular system. There is an increasing recognition that in healthy individuals the blood also harbors a diverse bacterial microbiota[34–36]. This new paradigm suggests that microbiota are present in the circulation from healthy conditions and may play a fundamental role for the maintenance of regulatory pathways involved in the immune tolerance. There are hundreds of bacterial products metabolites, co-metabolites (e.g. TMAO) released into the host circulation that can impact host physiology. It would be premature to conclude that any one of these bacterial products is responsible for the observed signaling to inactivate cofilin and promote actin polymerization. Some potential candidates to consider are bacterial N-formyl peptides (NFPs), such as formyl-methionyl-leucyl-phenylalanine (fMLP), which binds to formyl-peptide receptor-1 to induce actin polymerization[23]. Interestingly, it was demonstrated that blood levels of the microbiota-produced NFPs, formyl-methionyl-leucyl-phenylalanine (fMLP or fMLF; ~ 0.1 nM), are present in health animals, but they are exacerbated in obese mice[37]. Further, these authors also observed that treatment with antibiotics significantly decreased NFPs levels in both health and obese animals[37]. Others include microbial metabolites such as equol[38] or urolithin[39], both of which are known to regulate actin polymerization. It is more likely that more than one bacterial product or metabolite or cumulative effects of these metabolites is influencing the fundamental cytoskeletal dynamics of VSMCs of the host.

Several studies in mice, rats and humans have revealed a link between microbiota and host cardiovascular responses. The designs used for these studies included associations on the microbiota and BP based on the employment of antibiotics to clear pre-existing microbiota and/or microbial transplantations, along with correlations of bacterial taxa shifts in human hypertensive patients[10,12–14,31]. These designs are informative, but not perfect for examining cause-effect relationships between microbiota and host BP regulation. Germ-free models, by virtue of them being depleted of microbes, represent incomplete holobionts. Comparing these incomplete holobionts with microbial-reconstituted, and thereby complete holobionts, provided this study the platform to directly address the question of whether microbes are essential to maintain host cardiovascular homeostasis. The data generated, which

demonstrates that vascular contraction and BP of animals without microbiota are lower than the ones with microbiota, support our hypothesis that microbiota are essential for the host to maintain its hemodynamic homeostasis.

In summary, our findings show that the vascular system senses and responds to the presence of microbiota with a notable impairment in vascular contractility via enhanced actin depolymerization. We propose that this may be one of the potential mechanisms explaining how microbiota are mechanistically connected with BP homeostasis.

### Limitations of the study

The age of rats used in the present study (7 weeks old) is a limitation. These animals are in the developmental phase of their life when compared to ones as full adult (~12 weeks old). It is possible that different ages may present different vascular responses. Another limitation of the present study was that we were not able to use female rats. In our previous study, we observed that germ-free mice present sex-specific vascular remodeling in mice[32]. Specifically, it was observed that resistance arteries from male germ-free mice demonstrated increased vascular stiffness and inward hypotrophic remodeling, a characteristic of chronic reduction in blood flow. On the other hand, resistance arteries from germ-free female mice presented outward hypertrophic remodeling, a characteristic seen in aging[32].

### Perspectives

By comparing incomplete holobionts with complete holobionts, we support the previous studies that observed that reconstitution of microbiota has many benefits for the host. Therefore, scientists and physiologists should focus on the identification of the microbiota-derived molecule(s) which is(are) present in the blood, and may mediate physiological and pathophysiological changes in cardiovascular function.

## Supplementary Material

Refer to Web version on PubMed Central for supplementary material.

## Sources of Funding

This work was supported by the National Institutes of Health R00GM118885 (C.F. Wenceslau), R01HL143082 (B. Joe), R01CA219144 (M. Vijay-Kumar), K99HL151889 (C.G. McCarthy); the American Heart Association 18POST34060003 (C.G. McCarthy), National Science Foundation AGEP#1432878 (J.M. Edwards) and Biocodex Microbiota Foundation USA (T. Yang).

## References

1. Collaboration NCDRF. Long-term and recent trends in hypertension awareness, treatment, and control in 12 high-income countries: An analysis of 123 nationally representative surveys. Lancet. 2019;394:639–651 [PubMed: 31327564]
2. Muntner P, Carey RM, Gidding S, Jones DW, Taler SJ, Wright JT Jr., Whelton PK. Potential U.S. Population impact of the 2017 acc/aha high blood pressure guideline. J Am Coll Cardiol. 2018;71:109–118 [PubMed: 29146532]
3. Sabri M, Gheissari A, Mansourian M, Mohammadifard N, Sarrafzadegan N. Essential hypertension in children, a growing worldwide problem. J Res Med Sci. 2019;24:109 [PubMed: 31949460]

4. Devyatkin VA, Redina OE, Muraleva NA, Kolosova NG. Single-nucleotide polymorphisms (snps) both associated with hypertension and contributing to accelerated-senescence traits in oxys rats. Int J Mol Sci. 2020;21
5. Cheng X, Mell B, Alimadadi A, Galla S, McCarthy CG, Chakraborty S, Basrur V, Joe B. Genetic predisposition for increased red blood cell distribution width is an early risk factor for cardiovascular and renal comorbidities. Dis Model Mech. 2020;13
6. Rapp JP, Joe B. Dissecting epistatic qtl for blood pressure in rats: Congenic strains versus heterogeneous stocks, a reality check. Compr Physiol. 2019;9:1305–1337 [PubMed: 31688958]
7. Deng AY, Menard A. Biological convergence of three human and animal model quantitative trait loci for blood pressure. J Hypertens. 2020;38:322–331 [PubMed: 31584514]
8. Mell B, Cheng X, Joe B. Qtl mapping of rat blood pressure loci on rno1 within a homologous region linked to human hypertension on hsa15. PLoS One. 2019;14:e0221658 [PubMed: 31442284]
9. Warembourg C, Maitre L, Tamayo-Uria I, Fossati S, Roumeliotaki T, Aasvang GM, Andrusaityte S, Casas M, Cequier E, Chatzi L, Dedele A, Gonzalez JR, Grazuleviciene R, Haug LS, Hernandez-Ferrer C, Heude B, Karachaliou M, Krog NH, McEachan R, Nieuwenhuijsen M, Petraviciene I, Quentin J, Robinson O, Sakhi AK, Slama R, Thomsen C, Urquiza J, Vafeiadi M, West J, Wright J, Vrijheid M, Basagana X. Early-life environmental exposures and blood pressure in children. J Am Coll Cardiol. 2019;74:1317–1328 [PubMed: 31488269]
10. Mell B, Jala VR, Mathew AV, Byun J, Waghulde H, Zhang Y, Haribabu B, Vijay-Kumar M, Pennathur S, Bina Joe. Evidence for a link between gut microbiota and hypertension in the Dahl rat. Physiol Genomics. 2015;47(6):187–97. [PubMed: 25829393]
11. Galla S, Chakraborty S, Cheng X, Yeo JY, Mell B, Chiu N, Wenceslau CF, Vijay-Kumar M, Joe B. Exposure to Amoxicillin in Early Life Is Associated With Changes in Gut Microbiota and Reduction in Blood Pressure: Findings From a Study on Rat Dams and Offspring. J Am Heart Assoc. 2020 1 21;9(2):e014373. [PubMed: 31928175]
12. Marques FZ, Jama HA, Tsyganov K, Gill PA, Rhys-Jones D, Muralitharan RR, Muir J, Holmes A, Mackay CR. Guidelines for transparency on gut microbiome studies in essential and experimental hypertension. Hypertension. 2019;74:1279–1293 [PubMed: 31679421]
13. Adnan S, Nelson JW, Ajami NJ, Venna VR, Petrosino JF, Bryan RM Jr., Durgan DJ. Alterations in the gut microbiota can elicit hypertension in rats. Physiol Genomics. 2017;49:96–104. [PubMed: 28011881]
14. Yang T, Santisteban MM, Rodriguez V, Li W, Ahmari N, Carvajal JM, Zadeh M, Gong M, Qi Y, Zubcevic J, Sahay B, Pepine CJ, Raizada MK, Mohamadzadeh M. Gut Dysbiosis Is Linked to Hypertension. Hypertension. 2015;65(6):1331–40. [PubMed: 25870193]
15. Grundy D. Principles and standards for reporting animal experiments in The Journal of Physiology and Experimental Physiology. J Physiol. 2015; 593:2547–2549 [PubMed: 26095019]
16. Hagdorn QAJ, Bossers GPL, Koop AC, Piek A, Eijgenraam TR, van der Feen DE, Silljé HHW, de Boer RA, Berger RMF. A novel method optimizing the normalization of cardiac parameters in small animal models: The importance of dimensional indexing. Am J Physiol Heart Circ Physiol. 2019;316:H1552–H1557. [PubMed: 30978120]
17. Wostmann B, Brickner-Kardoss E. Development of cecal distention in germ-free baby rats. Am J Physiol. 1959;197:1345–6 [PubMed: 13846013]
18. Edgar RC. Search and Clustering Orders of Magnitude Faster Than BLAST. Bioinformatics. 2010;26(19):2460–1. [PubMed: 20709691]
19. Caporaso JG, Kuczynski J, Stombaugh J, Bittinger K, Bushman FD, Costello EK, Fierer N, Peña AG, Goodrich JK, Gordon JI, Huttley GA, Kelley ST, Knights D, Koenig JE, Ley RE, Lozupone VA, McDonald D, Muegge BD, Pirrung M, Reeder J, Sevinsky JR, Turnbaugh PJ, Walters WA, Widmann J, Yatsunenko T, Zaneveld J, Knight R. Nat Methods. 2010;7(5):335–6. [PubMed: 20383131]
20. DeSantis TZ, Hugenholtz P, Larsen N, Rojas M, Brodie EL, Keller K, Huber T, Dalevi D, Hu P, Andersen GL. Greengenes, a Chimera-Checked 16S rRNA Gene Database and Workbench Compatible With ARB. Appl Environ Microbiol. 2006;72(7):5069–72. [PubMed: 16820507]

21. Stanoszek LM, Crawford EL, Blomquist TM, Warns JA, Willey PF, Willey JC. Quality Control Methods for Optimal BCR-ABL1 Clinical Testing in Human Whole Blood Samples. J Mol Diagn. 2013;15(3):391–400. [PubMed: 23541592]
22. Wenceslau CF, Rossoni LV. Rostafuroxin ameliorates endothelial dysfunction and oxidative stress in resistance arteries from deoxycorticosterone acetate-salt hypertensive rats: the role of Na+K+-ATPase/ cSRC pathway. J Hypertens. 2014;32(3):542–54. [PubMed: 24309491]
23. Wenceslau CF, McCarthy CG, Szasz T, Calmasini FB, Mamenko M, Webb RC. Formyl peptide receptor-1 activation exerts a critical role for the dynamic plasticity of arteries via actin polymerization. Pharmacol Res. 2019;141:276–290. [PubMed: 30639374]
24. Mulvany MJ, Halpern W. Contractile properties of small arterial resistance vessels in spontaneously hypertensive and normotensive rats. Circ Res. 1977;41:19–26. [PubMed: 862138]
25. Zou J, Chassaing B, Singh V, Pellizzon M, Ricci M, Fythe MD, Kumar MV, Gewirtz AT. Fiber-Mediated Nourishment of Gut Microbiota Protects Against Diet-Induced Obesity by Restoring IL-22-Mediated Colonic Health. Cell Host Microbe. 2018;23(1):41–53.e4. [PubMed: 29276170]
26. Hrncir T, Stepankova R, Kozakova H, Hudcovic T, Tlaskalova-Hogenova H. Gut Microbiota and Lipopolysaccharide Content of the Diet Influence Development of Regulatory T Cells: Studies in Germ-Free Mice. BMC Immunol. 2008;9:65. [PubMed: 18990206]
27. Yang T, Chakraborty S, Saha P, Mell B, Cheng X, Yeo JY, Mei X, Zhou G, Mandal J, Golonka R, Yeoh BS, Putluri V, Piyarathna DWB, Putluri N, McCarthy CG, Wenceslau CF, Sreekumar A, Gewirtz AT, Vijay-Kumar M, Joe B. Gnotobiotic Rats Reveal That Gut Microbiota Regulates Colonic mRNA of Ace2, the Receptor for SARS-CoV-2 Infectivity. Hypertension. 2020;76(1):e1–e3. [PubMed: 32426999]
28. Park JS, Burckhardt CJ, Lazcano R, Solis LM, Isogai T, Li L, Chen CS, Gao B, Minna JD, Bachoo R, DeBerardinis RJ, Danuser G. Mechanical Regulation of Glycolysis via Cytoskeleton Architecture. Nature. 2020;578(7796):621–626. [PubMed: 32051585]
29. Sumi T, Matsumoto K, Takai Y, Nakamura T. Cofilin Phosphorylation and Actin Cytoskeletal Dynamics Regulated by Rho- And Cdc42-activated LIM-kinase 2. J Cell Biol. 1999;147(7):1519–32. [PubMed: 10613909]
30. Zheng K, Xiang Y, Wang X, Wang Q, Zhong M, Wang S, Wang X, Fan J, Kitazato K, Wang Y. Epidermal growth factor receptor-PI3K signaling controls cofilin activity to facilitate herpes simplex virus 1 entry into neuronal cells. mBio. 2014; 5(1):e00958–13 [PubMed: 24425731]
31. Li J, Zhao F, Wang Y, Chen J, Tao J, Tian G, Wu S, Liu W, Cui Q, Geng B, Zhang W, Weldon R, Auguste K, Yang L, Liu X, Chen L, Yang X, Zhu B, Cai J. Gut microbiota dysbiosis contributes to the development of hypertension. Microbiome. 2017;5:14. [PubMed: 28143587]
32. Edwards JM, Roy S, Tomcho JC, Schreckenberger ZJ, Chakraborty S, Bearss NR, Saha P, McCarthy CG, Vijay-Kumar M, Joe B, Wenceslau CF. Microbiota Are Critical for Vascular Physiology: Germ-free Status Weakens Contractility and Induces Sex-Specific Vascular Remodeling in Mice. Vascul Pharmacol. 2020;125–126.
33. Staiculescu MC, Galiñanes E, Zhao G, Ulloa U, Jin M, Beig MI, Meininger GA., Martinez-Lemus LA. Prolonged vasoconstriction of resistance arteries involves vascular smooth muscle actin polymerization leading to inward remodelling. Cardiovasc Res. 2013;98:428–36. [PubMed: 23417038]
34. Castillo DJ, Rifkin RF, Cowan DA, Potgieter M. The Healthy Human Blood Microbiome: Fact or Fiction? Front Cell Infect Microbiol. 2019;9:148. [PubMed: 31139578]
35. Bahrani-Mougeot FK, Paster BJ, Coleman S, Ashar J, Barbuto S, Lockhart PB. Diverse and novel oral bacterial species in blood following dental procedures. J. Clin. Microbiol 2008;46:2129–2132. [PubMed: 18434561]
36. Païssé S, Valle C, Servant F, Courtney M, Burcelin R, Amar J, Lelouvier B. Comprehensive description of blood microbiome from healthy donors assessed by 16S targeted metagenomic sequencing. Transfusion. 2016;56:1138–1147. [PubMed: 26865079]
37. Wollam J, Riopel M, Xu YJ, Johnson AMF, Ofrecio JM, Ying W, El Ouarrat D, Chan LS, Han AW, Mahmood NA, Ryan CN, Lee YS, Watrous JD, Chordia MD, Pan D, Jain M, Olefsky JM. Microbiota-Produced N-Formyl Peptide fMLF Promotes Obesity-Induced Glucose Intolerance. Diabetes. 2019;68(7):1415–1426. [PubMed: 31010956]

38. Harada K, Sada S, Sakaguchi H, Takizawa M, Ishida R, Tsuboi T. Bacterial Metabolite S-equol Modulates Glucagon-Like peptide-1 Secretion From Enteroendocrine L Cell Line GLUTag Cells via Actin Polymerization. Biochem Biophys Res Commun. 2018;501(4):1009–1015. [PubMed: 29777703]

39. Alauddin M, Okumura T, Rajaxavier J, Khozooei S, Pöschel S, Takeda S, Singh Y, Brucker SY, Wallwiener D, Koch A, Salker MS. Gut Bacterial Metabolite Urolithin A Decreases Actin Polymerization and Migration in Cancer Cells. Mol Nutr Food Res. 2020;64(7):e1900390. [PubMed: 31976617]

## Novelty and Significance

**What Is New?**

- This is the first report using conventionalized GF rats to study the contributions of microbiota to vascular function and BP regulation in healthy animals;
- This is the first study to observed that reduced actin polymerization, via cofilin activation, is the cause of vascular hypocontractility in GF rats.

**What Is Relevant?**

- In light of the insufficient mechanistic data and cause-effect relationship on microbiota and cardiovascular system, our results are relevant because indicate that the vascular system senses the presence (or lack of) microbiota to maintain vascular tone.
- In the absence of dysbiosis, microbiota are not pathological in inducing abnormal elevation BP.

**Summary**

Introducing microbiota for a short duration of 10 days was enough to elicit differential vascular and BP responses, suggesting that microbial factor(s) cause rapid effects on the host cardiovascular system. Taken together, these results constitute a fundamental discovery of the essential nature of microbiota in BP regulation.

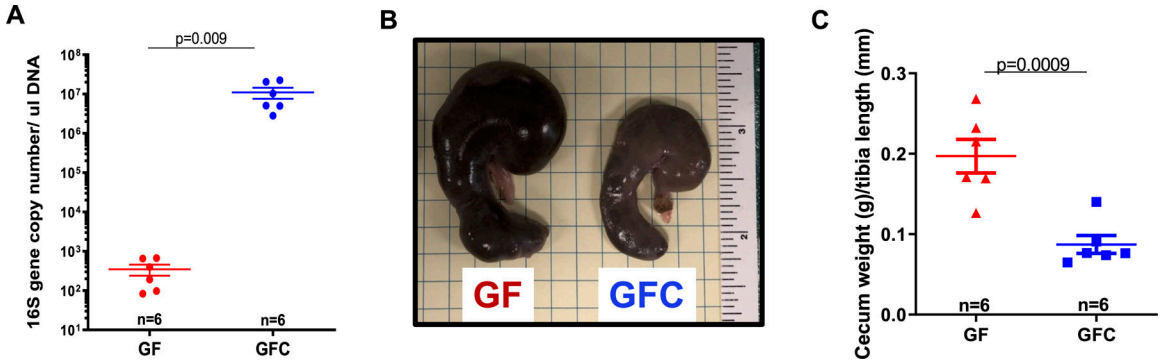


**Figure 1.**

16S ribosomal RNA (rRNA) gene sequencing and analysis from fecal DNA extracted from one fecal pellet (A). Representative image (B) and cecum weight (C) from male 7-week-old Sprague Dawley (SD) rats that were either germ-free (GF) or germ-free conventionalized (GFC). Number of animals and p values are indicated in the graphs. Data are presented as mean ± SEM. Student's t test; *vs. GF. $p<0.05$.

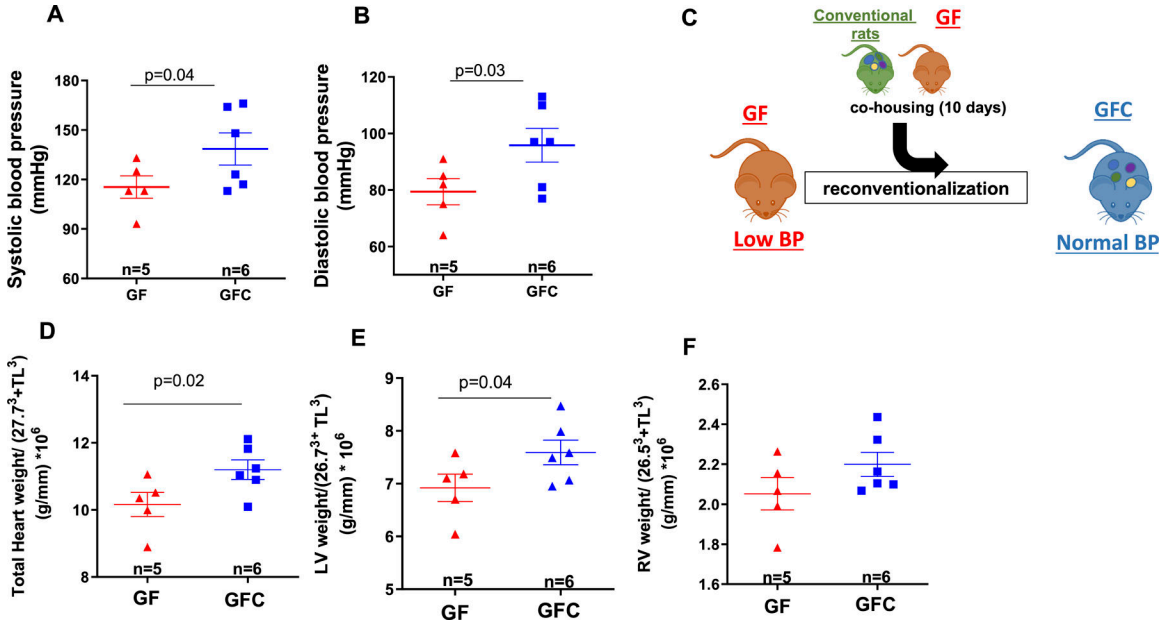


**Figure 2.**

Systolic (A) and diastolic (B) blood pressure measurements. Illustration (C) shows co-housing of male 7-week-old Sprague Dawley (SD) rats that were either germ-free (GF) or germ-free conventionalized (GFC). Total heart (D), left (LV, E) and right (RV, F) ventricular weight normalized by $27.7^3$ + tibia length$^3$ (TL); $26.7^3$ + tibia length$^3$ (TL) and $26.5^3$ + tibia length$^3$ (TL) respectively. Number of animals and p values are indicated in the graphs. Data are presented as mean ± SEM. Student's t test; $p<0.05$.

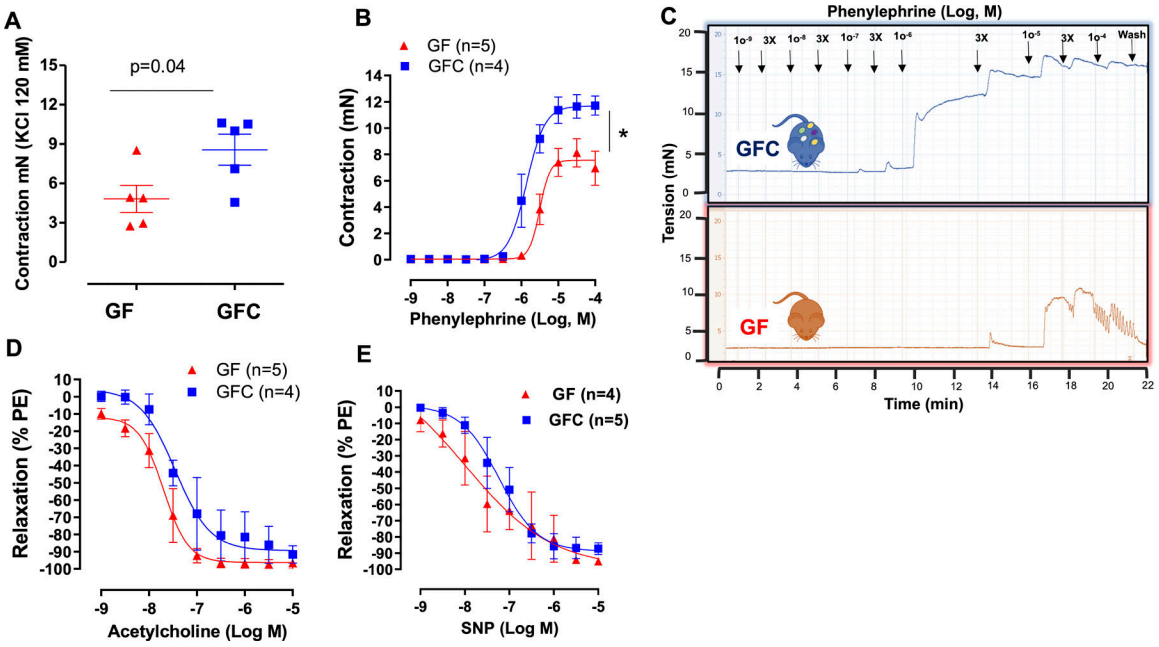


**Figure 3.**

Contraction to KCl (120 mmol/L) (A) and concentration response curves to phenylephrine (B and C), acetylcholine (D) or sodium nitroprusside (SNP) (E) in mesenteric resistance arteries (MRA) from male 7-week-old Sprague Dawley (SD) rats that were either germ-free (GF) or germ-free conventionalized (GFC). For relaxation curves, arteries were contracted with phenylephrine (10 μmol/L). Number of animals and p values are indicated in the graphs. Data are presented as mean ± SEM. Two-way ANOVA or Student's t test; *vs. GF. $p<0.05$.

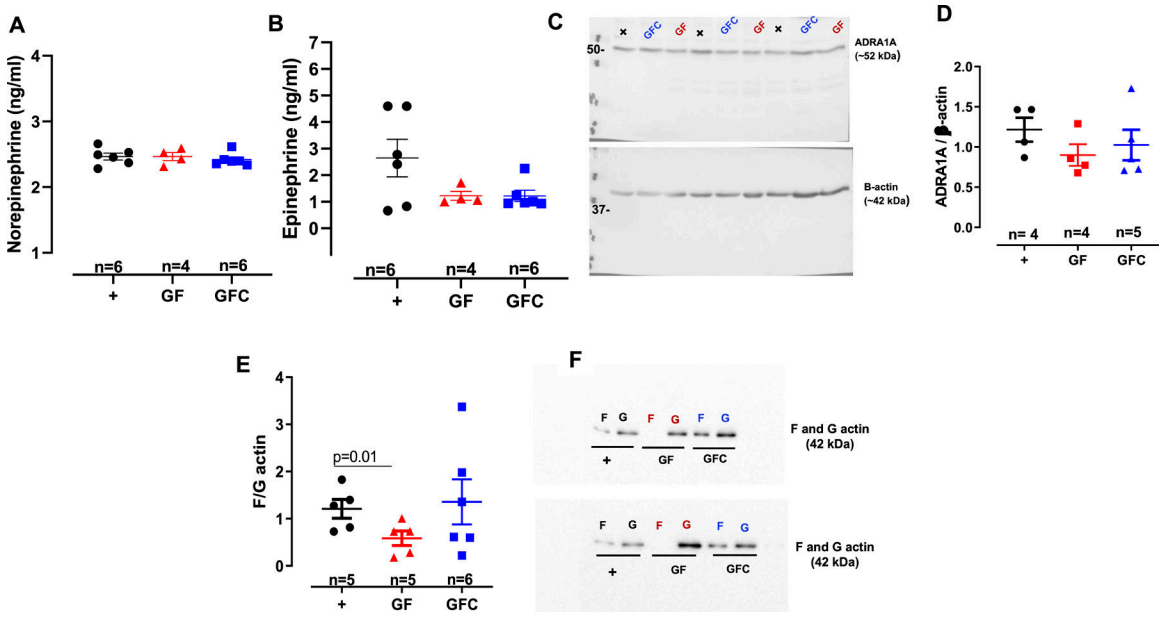


**Figure 4.**

Plasma noradrenaline (norepinephrine) (A) and adrenaline (epinephrine) (B) concentrations. Densitometric analysis and representative images of immunoblots from alpha-1a adrenergic receptor (ADRA1A) and β-actin (C and D) and filamentous F-to-globular G-actin ratio (E and F) in vascular smooth muscle cells (VSMCs) from male 7-week-old Sprague Dawley [(SD, positive control (+)] rats, SD rats that were germ-free (GF) or germ-free conventionalized (GFC). Number of animals and p values are indicated in the graphs. Data are presented as mean ± SEM. One-way ANOVA or Student's t test.

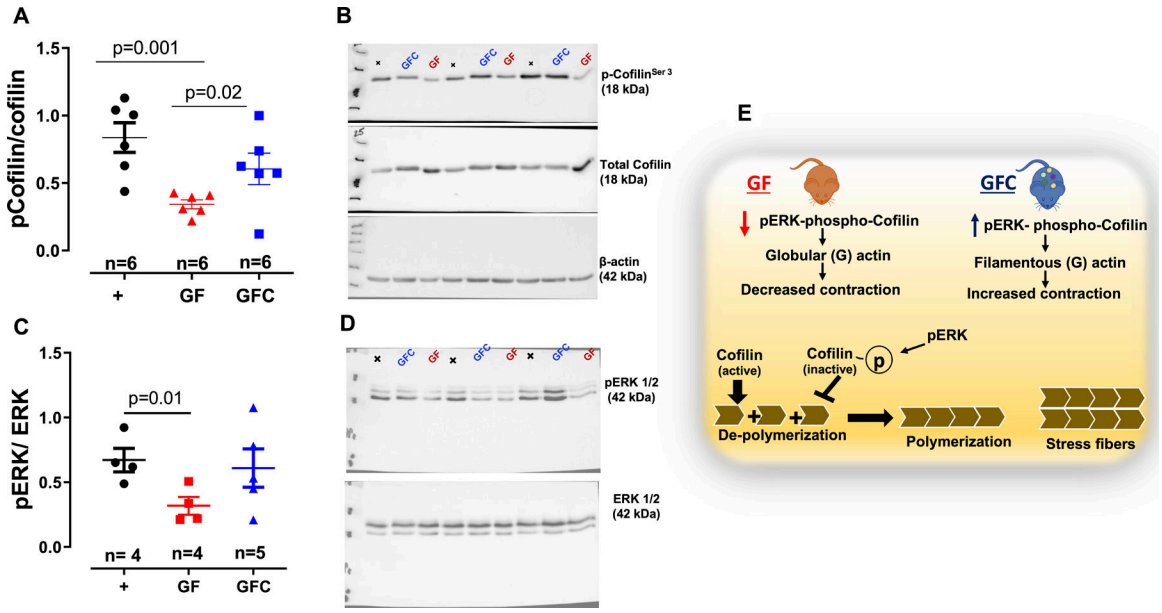


**Figure 5.**

Densitometric analysis and representative images of immunoblots from total and phospho cofilin (A and B) and ERK1/2 (C and D) in vascular smooth muscle cells (VSMCs) from male 7-week-old Sprague Dawley [(SD, positive control (+)] rats, SD rats that were germ-free (GF) or germ-free conventionalized (GFC). Illustration (E) shows that acquisition of microbiota in GFC rats, ERK 1/2 phosphorylates and inactivates the actin-depolymerizing protein cofilin leading to a stabilization of actin stress fibers to maintain vascular tone. Number of animals and p values are indicated in the graphs. Data are presented as mean ± SEM. One-way ANOVA or Student's t test.

**Table 1:**

Body and organ weight

| | GF | GFC | *t-test* vs. GF |
|---|---|---|---|
| **Body weight (g)** | 205.7 ± 12 (n=6) | 262.8 ± 5* (n=6) | p=0.001 |
| **Kidney weight /tibia length (g/mm)** | 0.048 ± 0.001 (n=6) | 0.052 ± 0.001 (n=5) | p >0.05 |
| **Spleen weight /tibia length (g/mm)** | 0.013 ± 0.001 (n=6) | 0.015 ± 0.0004 (n=6) | p >0.05 |
| **White adipose tissue (g)** | 0.77 ± 0.13 (n=6) | 1.12 ± 0.06* (n=6) | p=0.04 |